

# Detection of multiple fluorescent dyes using liquid crystal variable retarder and sparse modeling

Kazuma Fujiwara.<sup>1</sup>, Takuya Funatomi.<sup>1</sup>, Kazuya Kitano.<sup>1</sup>, Yuki Fujimura.<sup>1</sup>, Yasuhiro Mukaigawa.<sup>1</sup>, Hiroshi Ochiai.<sup>2</sup>; <sup>1</sup> Nara Institute of Science and Technology, Ikoma, Nara, Japan 630–0192; <sup>2</sup> Kyushu University, Fukuoka, Japan, 812–0054.

## Abstract

*In spatial transcriptomics, which allows the analysis of gene expression while preserving its location in tissues, RNA molecules are hybridized with a fluorescent-labeled DNA probe for detection. In this study, we aim to improve the efficiency of spatial transcriptomics by simultaneously using multiple fluorescent dyes with overlapping spectra. We propose a method to quantify each fluorescent dyes using a liquid crystal variable retarder as a spectral modulator, which can control the spectral transmittance by changing the voltage. The spectrum of light passing through the modulator is integrated by the image sensor and observed as intensity. We quantify the fluorescent dyes at each pixel using intensities of various spectral transmittances as a spectral code and applying sparse modeling using a dictionary created by simulating observations for the fluorescent dyes used in hybridization. We verified the principle of the proposed method and demonstrated its feasibility through simulation experiments.*

## Introduction

RNA sequencing (RNA-seq) has greatly advanced biology by providing gene expression data for entire tissues and cell populations. In contrast, spatial transcriptomics is a new approach that maps gene expression while preserving its location in tissues, which provides spatially richer information than previous RNA-seq (Fig. 1). This enables a more detailed understanding of cellular behavior in vivo and is being applied in fields such as developmental biology and drug discovery. To perform high-resolution spatial transcriptomics and detect numerous RNA molecular species, previous methods such as seqFISH [1] require multiple cycles of hybridization and reprobings of fluorescent-labeled DNA probes to target RNA molecules. It generally uses three different fluorescent channels, and for each channel, it repeats 20 rounds of DNA probe hybridization, fluorescence detection by microscopy, and four rounds of reprobings. By using one round for error correction, the method can detect up to 24,000 different RNA molecular species. However, the procedure requires a total of 80 rounds of hybridization and image acquisition, with each round taking approximately an hour. Notably, after every set of ten hybridizations, manual experimental manipulations are necessary. Therefore, this repetitive process is time-consuming and labor-intensive.

If many fluorescent dyes can be used simultaneously, the number of hybridizations and reprobings can be reduced, thereby improving the efficiency of the analysis. However, due to the limitation of overlapping fluorescence spectra, general fluorescence microscopes can use only a few types of fluorescent dyes at most.

The objective of this study is to develop a method that can stably detect multiple fluorescent dyes without being affected by

the overlapping spectra of fluorescent dyes. This is expected to enable high-throughput seqFISH analysis of a larger number of RNA molecular species with fewer rounds than the existing seqFISH [1]. Looking back at the progress of genome analysis, it has greatly stimulated biological research by achieving speed and cost reduction. Based on this, spatial transcriptomics will become easier if seqFISH is made high-throughput in this study. As a result, it is expected that the whole research field will be further stimulated.

## Related work

### Fluorescence detection methods

Fluorescence is a phenomenon in which fluorescent dyes are excited by light of shorter wavelengths and then emit it as light of longer wavelengths.

A fluorescence microscope is an instrument that uses this fluorescence phenomenon to illuminate the sample with light of a specific wavelength that passes through an excitation filter and observes the emission wavelength selected by a barrier filter [2]. Instead of an excitation filter, lasers are also often used. These filters are bandpass filters that allow only light in a specific wavelength range to pass through. When using multiple fluorescent dyes, the fluorescence from a specific dye can be clearly obtained by selecting and switching the excitation and barrier filters that match each dye. However, crosstalk due to overlapping spectra between fluorescent dyes makes it difficult to detect multiple fluorescent dyes simultaneously. Therefore, the fluorescent dyes used simultaneously should be chosen so that their spectra do not overlap. SeqFISH [1] described above uses this method to detect three different fluorescent dyes.

The most naïve method to detect more fluorescent dyes is to observe fluorescence using hyperspectral imaging, which can capture spectra in detail. Hyperspectral imaging measures spectral cubes, which are three-dimensional data consisting of two-dimensional intensity images at different wavelengths.

There are many variations of this technique [3], but the most

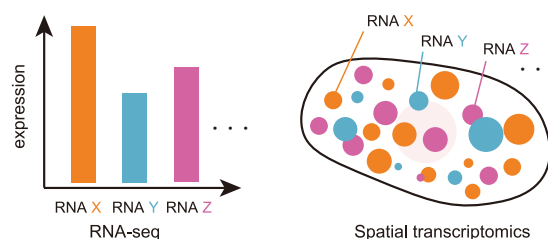


Figure 1. RNA-seq and spatial transcriptomics.

common method is to use a spectrometer or similar device to split the light emitted by a dye into narrow wavelength bands and construct a spectral cube. Timo *et al.* has also proposed a method for detection and separation of fluorescent dyes by linear separation based on the obtained spectral cube [4, 5].

However, as the number of spectral channels increases to enhance wavelength resolution in hyperspectral imaging, each channel captures less light, leading to a decrease in signal strength. This reduced signal strength, in combination with consistent background noise, results in a lower signal-to-noise ratio. This phenomenon is particularly challenging when attempting to detect weak fluorescence signals, a common issue in high-throughput seqFISH. For high-throughput seqFISH, high-speed imaging is essential, but this often exacerbates the challenge of accurately detecting weak fluorescence signals. The faster imaging speed, necessary for throughput, can increase the relative impact of noise, thereby diminishing the precision of fluorescent dye detection.

### Spectral Imaging with Liquid Crystal Variable Retarder

There is coded sensing that achieves better sensitivity by indirect sensing instead of direct spectral measurement. For example, by using a spectral modulator consisting of a liquid crystal variable retarder and two polarizers, we can retain about 40% of the fluorescence intensity. This can suppress the effect of noise. August *et al.* used a liquid crystal variable retarder in front of an image sensor and compressed sensing for hyperspectral imaging [6]. Their method is similar to ours in using a liquid crystal variable retarder as a spectral modulator. In this method, a spectral cube with about 0.4 nm resolution (1000 channels) in 400 nm to 800 nm bandwidth is reconstructed from 100 observations. In addition, Yang *et al.* proposed a method for hyperspectral imaging by attaching a liquid crystal variable retarder to the illumination to incorporate this mechanism into a microscope [7]. A spectral cube with 0.6 nm resolution (345 channels) in the 460 nm to 660 nm bandwidth is reconstructed from 50 observations. Since both methods reconstruct the spectral cube, it is possible to quantify multiple fluorescent dyes with spectral overlap. However, in reality, the number of fluorescent dyes used simultaneously is about several dozen at most, and the reconstruction of 345 channels is excessive; it is expected that the direct quantification of fluorescent dyes can provide noise-robust quantification from a small number of observations, rather than quantifying fluorescent dyes after the reconstruction of the spectral cube.

### Method

In this study, we propose a method for directly quantifying multiple fluorescent dyes without reconstructing the spectral cube by combining fluorescence observation using a spectral modulator and sparse modeling techniques (Fig. 2). This method consists of two processes: spectral encoding, which encodes the input through a spectral modulator, and dye decoding, which quantifies fluorescent dyes based on the obtained code. Since both encoding and decoding are pixel independent, all the process are executed in parallel.

#### Spectral encoding

The spectral modulator consists of a Liquid Crystal Variable Retarder (LCVR) and two polarizers. The LCVR is oriented at

45° to the axis of the polarizers. The spectral transmittance of the spectral modulator can be modulated according to the voltage applied to the LCVR as

$$t(\lambda, V_k) \propto \frac{1}{2} - \frac{1}{2} \cos\left(\frac{\Delta n(V_k, \lambda)d}{\lambda}\right), \quad (1)$$

where  $\lambda$  is the wavelength,  $d$  is the thickness of LCVR,  $\Delta n(V_k, \lambda)d$  is the birefringence at LCVR voltage  $V_k$  and  $\lambda$  [8]. Also,  $\frac{\Delta n(V_k, \lambda)d}{\lambda}$  is the amount of phase difference of LCVR and is called retardance.

When a spectral modulator is placed in front of the sensor, the spectral distribution incident on the image sensor becomes the multiplication of the spectral distribution of the fluorescent-labeled targets, the spectral sensitivity characteristics of the sensor, and the spectral transmittance of the spectral modulator. Then, the intensity observed by the sensor is obtained by integrating it over the observable range. Here, the intensity on the sensor at a given voltage  $V_k$  is described by

$$i_k = \int f(\lambda)t(\lambda, V_k)s(\lambda)d\lambda, \quad (2)$$

where  $f(\lambda)$  is the spectral distribution of fluorescent-labeled targets and  $s(\lambda)$  is the spectral sensitivity characteristic of the sensor.

This intensity  $i_k$  varies with voltage, and by changing the voltage  $N$  times, we can obtain an  $N$ -dimensional spectral code that is unique to the input spectral distribution. The  $N$ -dimensional spectral code is described by

$$\mathbf{i} = [i_1 \quad \cdots \quad i_k \quad \cdots \quad i_N]^T. \quad (3)$$

#### Dye decoding

The spectral distribution of fluorescent-labeled targets can be expressed as a linear combination of the contributing fluorescent dyes [9] and described by

$$f(\lambda) = \sum_{j=1}^P c_j r_j(\lambda), \quad (4)$$

where  $P$  is the number of different fluorescent dyes present in the whole sample,  $j = 1, 2, \dots, P$  represents the index of the fluorescent dye,  $c_j$  and  $r_j(\lambda)$  represents the concentration and the emission spectra of  $j$ -th fluorescent dyes, respectively. From Eq. (2), the intensity on the sensor is described by

$$i_k = \sum_{j=1}^P c_j \int r_j(\lambda)t(\lambda, V_k)s(\lambda)d\lambda. \quad (5)$$

From Eq. (3), the  $N$ -dimensional spectral code is described by

$$\begin{aligned} \mathbf{i} &= \begin{bmatrix} d_{1,1} & \cdots & d_{1,P} \\ \vdots & \ddots & \vdots \\ d_{N,1} & \cdots & d_{N,j} \end{bmatrix} \begin{bmatrix} c_1 \\ \vdots \\ c_P \end{bmatrix} \\ &= \mathbf{D}\mathbf{c}, \end{aligned} \quad (6)$$

where  $d_{k,j} = \int r_j(\lambda)t(\lambda, V_k)s(\lambda)d\lambda$ .  $\mathbf{D}$  can be computed if  $r_j(\lambda)$  is known. Since the spectral distribution of fluorescent dyes is generally known,  $\mathbf{D}$  can be composed as

$$\mathbf{D} = [\mathbf{d}_1 \quad \cdots \quad \mathbf{d}_j \quad \cdots \quad \mathbf{d}_P], \quad (7)$$

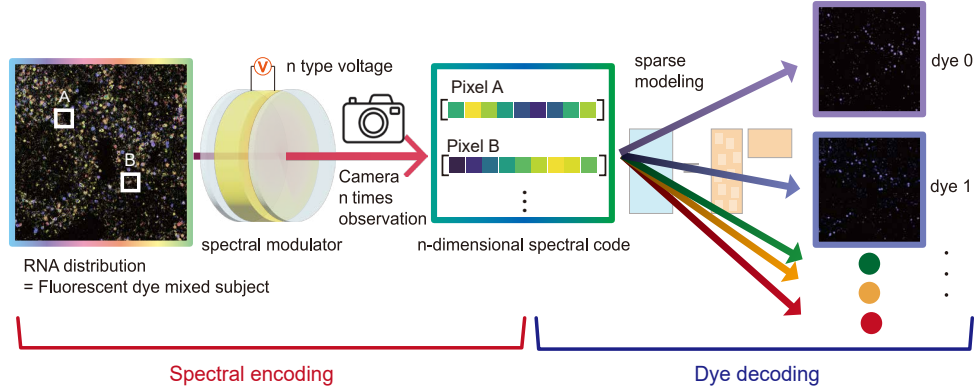


Figure 2. Outline of the proposed method.

where  $\mathbf{d}_j$  is  $\mathbf{i}$  when only the  $j$ -th dye is present at unit concentration and no other dyes are present. This is the  $N$ -dimensional spectral code of a single dye. In this paper,  $\mathbf{d}_j$  is called a dye code. Equation (6) shows that the  $N$ -dimensional spectral code  $\mathbf{i}$  can be expressed as a linear combination of the weights  $c_j$  and the dye codes  $\mathbf{d}_j$ .

Figure 3 shows that different dye codes can be obtained even for the dyes with close peaks or the dyes with identical peak values but different spectral widths in their fluorescence spectra (see the next section for the details on voltage settings).

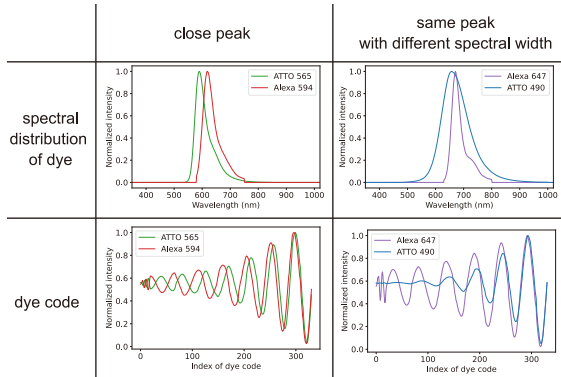


Figure 3. Different dye codes are generated depending on the spectral distribution.

Since we can naturally assume that the number of fluorescent dyes observed simultaneously is small, sparse modeling is an appropriate method to quantify their concentrations. Therefore, we can use  $\mathbf{D}$  as a dictionary for sparse modeling using Lasso Lars [10] and obtain the following formulation:

$$\operatorname{argmin}_{\mathbf{c}} \left( \frac{1}{2} \|\mathbf{i} - \mathbf{D}\mathbf{c}\|_2^2 + \alpha \|\mathbf{c}\|_1 \right), \quad (8)$$

where  $\alpha$  is the regularization parameter. The optimization assumes that the sparsity of  $\mathbf{c}$  is larger as  $\alpha$  increases.

### Verification of the principle by simulation

We performed a simulation of observation based on fluorescence images obtained by seqFISH to verify the principle.

The spectral transmittance of the spectral modulator  $t(\lambda, V_k)$  is expressed by Eq. (1), but it cannot be calculated because the birefringence coefficient  $\Delta n(V_k, \lambda)d$  is unknown. Therefore, we measured the spectral transmittance experimentally. We used Thorlabs LCC1115-A as the LCVR and Thorlabs WP25M-VIS visible wire grid polarizer as the polarizer, and measured the transmittance using a spectrometer (Ocean Optics Maya2000 Pro). The voltage  $V_k$  applied to the LCVR affects the change in spectral transmittance. Considering this change, we selected 331 voltage values. By referring the retardance data of LCC1115-A at 633 nm and 25 °C published by Thorlabs, we selected the voltage so that the change in retardance was constant within the voltage resolution of the function generator (Rigol DG4162). We expected that this method would provide a more varied spectral transmittances than simply selecting equally spaced voltage values. In fact, as shown in the spectral response maps (Fig. 4), the variation in spectral transmittance was almost constant. In the spectral measurement, the spectral transmittance  $t(\lambda, V_k)$  was multiplied by the spectral sensitivity characteristics of the sensor of Maya2000 Pro. For the sake of simplicity, we assumed that the spectral sensitivity characteristics of the camera  $s(\lambda)$  were the same as those of Maya2000 Pro. We performed the simulation under this assumption.

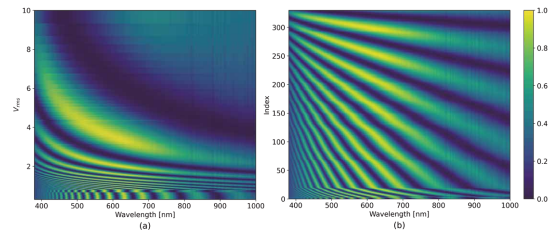


Figure 4. (a): Spectral response map with voltage on the vertical axis. Each column shows the spectral transmittance at a given voltage. This map represents that the spectral transmittance varies little at high voltages. (b): Spectral response map with index as the vertical axis. Each column shows the spectral transmittance at a given index. The variation in spectral transmittance was almost constant among the voltage values.

In real fluorescence observation, the fluorescence signal consists not only of fluorescent spots from RNA molecules, but also of autofluorescence. To simulate this situation, we took the fol-

lowing steps. First, we prepared seven types of fluorescence images for different RNA molecule species and used them as ground truth. We chose the Alexa647 fluorescent dye image because it had less autofluorescence interference. However, since there was still some autofluorescence in this image, we removed it by applying a threshold determined by the Elbow method [11]. Next, we added different fluorescent dyes to each RNA molecule fluorescence image and calculated the intensity values observed through the spectral modulator using Eq. (2). The fluorescent dyes we used were Alexa 488, Alexa 594, Alexa 565, Alexa 647, Alexa 700, and ATTO 490. We also added Gaussian noise with a mean of 0 and a standard deviation of 1% of the intensity values to simulate the noise in the fluorescence observation. We used the proposed method to quantify the fluorescent dyes from the simulated images.

Figure 5 shows the reconstruction results using all 331 observations. Due to the nature of the dye codes (Fig. 3), the PSNR of the quantification results obtained by the proposed method were sufficiently high compared to the ground truth, demonstrating that the proposed method can effectively quantify the fluorescent dyes. We also varied the value of  $\alpha$  in Eq. (8) and selected the one that maximized the mean of the PSNR for the seven fluorescent dyes. We found that the reconstruction accuracy was improved by imposing an appropriate sparsity constraint (Fig. 6).

dye	ground truth	our method	PSNR
ATTO 490			69.61
Alexa 488			77.57
ATTO 565			66.22
Alexa 594			71.65
Alexa 647			68.97
Alexa 700			76.40
Alexa 750			75.44

**Figure 5.** Results of fluorescence quantification simulation. (all 331 observations)

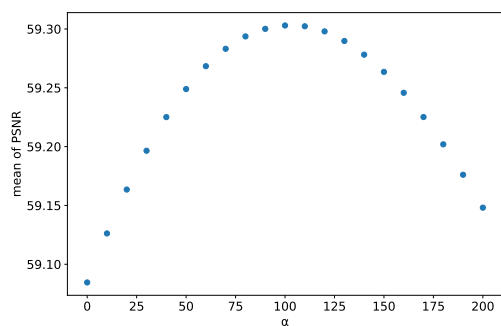


**Figure 6.** Mean of PSNR for seven fluorescent dyes. Varying  $\alpha$  changes the reconstruction accuracy.  $\alpha = 100$  is optimal.

To further improve efficiency and examine how the reconstruction quality changes with different numbers of observations,

we performed a simulation in which we randomly selected a fixed number of observations from the original 331. As a result, we observed a trade-off between the number of observations and reconstruction quality (Fig. 7).

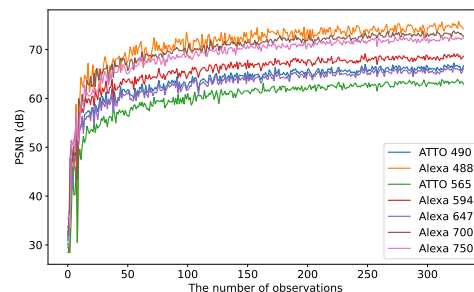


**Figure 7.** A trade-off between the number of observations and reconstruction quality.

dye	ground truth	our method	PSNR
ATTO 490			58.74
Alexa 488			67.64
ATTO 565			55.59
Alexa 594			61.32
Alexa 647			57.78
Alexa 700			65.05
Alexa 750			63.57

**Figure 8.** Results of fluorescence quantification simulation (25 observation points equally spaced from the original 331 points)

Figure 8 shows the reconstruction results when we used 25 observation points equally spaced from the original 331 points.

## Conclusion

In this study, we proposed a method for quantifying multiple fluorescent dyes by combining fluorescence observation with a spectral modulator and sparse modeling techniques. This method assumes that the spectral distribution of the fluorescent dyes is known, and quantifies the concentration of each dye by modeling the observed values as a linear combination of dye codes that are unique to each dye. We performed a simulation experiment based on the fluorescence images obtained by seqFISH. As a result, seven fluorescent dyes were quantified using the proposed method. We also examined the trade-off between the number of observations and the reconstruction quality by reducing the number of observations. We found that the reconstruction quality was still high when the number of observations was reduced from 331 to 25. This number of observations is smaller than the number of observations of 50 in the previous study [7], which used an LCVR to reconstruct the spectral cube, demonstrating the advantage of the proposed method. However, the proposed method still has room for improvement in the selection of spectral transmittance and fluorescent dyes. Therefore, as a future direction, we

aim to optimize the selection of spectral transmittance and fluorescent dyes, and to develop a method that can reliably detect RNA molecules with fewer observations and computations. Another future challenge is to validate the proposed method on real devices. We expect that the proposed method will enable fast and accurate analysis of a large number of RNA molecular species in the field of spatial transcriptomics.

## Acknowledgments

This work was partly supported by JST PRESTO JPMJPR2025 and JST CRESTO JPMJCR23N3.

## References

- [1] Eng, C.-H. L., Lawson, M., Zhu, Q., Dries, R., Koulena, N., Takei, Y., Yun, J., Cronin, C., Karp, C., Yuan, G.-C., and Cai, L.: Transcriptome-scale super-resolved imaging in tissues by RNA seq-FISH+. *Nature* 568, 235–239 (2019)
- [2] Lichtman, J. W. and Conchello, J.-A.: Fluorescence microscopy. *Nature Methods* 2, 910–919 (2005)
- [3] Hagen, N. A. and Kudenov, M. W.: Review of snapshot spectral imaging technologies. *Optical Engineering* 52, 090901 (2013)
- [4] Renkoski, T. E., Utzinger, U., and M.D., K. D. H.: Wide-field spectral imaging of human ovary autofluorescence and oncologic diagnosis via previously collected probe data. *Journal of Biomedical Optics* 17, 036003 (2012)
- [5] Li, Q., He, X., Wang, Y., Liu, H., Xu, D., and Guo, F.: Review of spectral imaging technology in biomedical engineering: achievements and challenges. *Journal of Biomedical Optics* 18, 100901 (2013)
- [6] August, I., Oiknine, Y., AbuLeil, M., Abdulhalim, I., and Stern, A.: Miniature Compressive Ultra-spectral Imaging System Utilizing a Single Liquid Crystal Phase Retarder. *Scientific Reports* 6 (2016)
- [7] Yang, T., Xu, Z., Ren, W., Feng, Y., Wu, D., Zhang, R., and Xie, Y.: Compressive hyperspectral microscopic imaging using spectral-coded illumination. *Optics & Laser Technology* 166, 109631 (2023)
- [8] Yariv, A. and Yeh, P.: *Optical waves in crystals*. Pure & Applied Optics S. John Wiley & Sons, Nashville, TN (1984)
- [9] Dickinson, M., Bearman, G., Tille, S., Lansford, R., and Fraser, S.: Multi-Spectral Imaging and Linear Unmixing Add a Whole New Dimension to Laser Scanning Fluorescence Microscopy. *BioTechniques* 31, 1272–1278 (2001)
- [10] Pedregosa, F., Varoquaux, G., Gramfort, A., Michel, V., Thirion, B., Grisel, O., Blondel, M., Prettenhofer, P., Weiss, R., Dubourg, V., et al.: Scikit-learn: Machine learning in Python. *Journal of Machine Learning Research* 12, 2825–2830 (2011)
- [11] Imbert, A., Ouyang, W., Safieddine, A., Coleno, E., Zimmer, C., Bertrand, E., Walter, T., and Mueller, F.: FISH-quant v2: a scalable and modular tool for smFISH image analysis. *RNA* 28, 786–795 (2022)